Acta Vulcanologica - Vol. 7 (2) – 1995: 43 - 52

Low-pressure evolution of magmas from the Călimani, Gurghiu and Harghita Mountains, East Carpathians

P. R.D. Mason[1]*, H. Downes[1], I. Seghedi[2], A. Szakács[2], M. F. Thirlwall[3]

1. *Research School of Geological and Geophysical Sciences, Birkbeck and University Colleges, Gower Street, London, WC1E 7HX, United Kingdom*
2. *Geological Institute of Romania, Str. Caransebes 1, RO-78344 Bucharest 32, Romania*
3. *Department of Geology, Royal Holloway University of London, Egham Hill, Egham, Surrey, TW20 OEX, United Kingdom*

Abstract

Calc-alkaline to high-K calc-alkaline volcanism took place in the Călimani, Gurghiu and Harghita Mountains of Romania between the late Miocene and the Pleistocene. Magmatism was related to the subduction of the European plate to the west and the south-west beneath the Tisza-Dacia microplate. A succession of 18 major volcanic centres is recognised along the arc segment for approximately 200km from north to south. Eruptive products were dominated by two-pyroxene andesites but lithologies from basalt to rhyolite are identified within individual volcanoes.

Fractional crystallisation of plagioclase, pyroxenes, amphibole and Fe-Ti oxides controlled major and compatible trace element chemistry in most volcanic centres. Amphibole is a major crystallising phase in more evolved andesites and dacites. Modelling is presented to quantify the role of fractionation in several volcanic centres. Mixing of magmas was an important process on both a macroscopic and microscopic scale including the dispersal of xenocrysts throughout host magmas. Crustal assimilation can be deduced from petrographic evidence and is supported by major element modelling.

1. Introduction

The Călimani, Gurghiu and Harghita Mountains (CGH) represent the final burst of calcalkaline magmatism in the Inner Carpathian arc. The CGH province contains 18 major volcanic centres which were active over a period of approximately 10Ma from the late Miocene into the Quaternary (Pécskay et al., 1995). The oldest volcanism took place in the north of the segment and the focus of magmatic activity shifted southwards, along the arc, with time.

The CGH volcanic province forms the most recent segment of the Inner Carpathian calc-alkaline arc and can be divided into four geographical units (Fig. 1). From north to south These are the Călimani, Gurghiu, Northern Harghita and Southern Harghita Mountains. Volcanism was active from the late Miocene into the early Pliocene in Călimani (Pécskay et al., 1995). The Gurghiu and Northern Harghita arc segments were active from the late Miocene into the Pliocene (Szakács et al., 1993b; Pécskay et al., 1995) and the youngest magmatism occurred in the Southern Harghita Mountains from the Pliocene into the Pleistocene (Peltz et al., 1985; Szakács et al., 1993a,b; Pécskay et al., 1995). The tectonic setting of the CGH arc is discussed in more detail elsewhere (Csontos et al., 1992; Szabó et al., 1992; Rădulescu & Săndulescu, 1973; Csontos, 1995).

Here we present mineral compositions and new major and trace element data for calc-alkaline rocks from the CGH volcanic province. The roles of fractional crystallisation, magma mixing, crystal accumulation and crustal contamination are addressed.

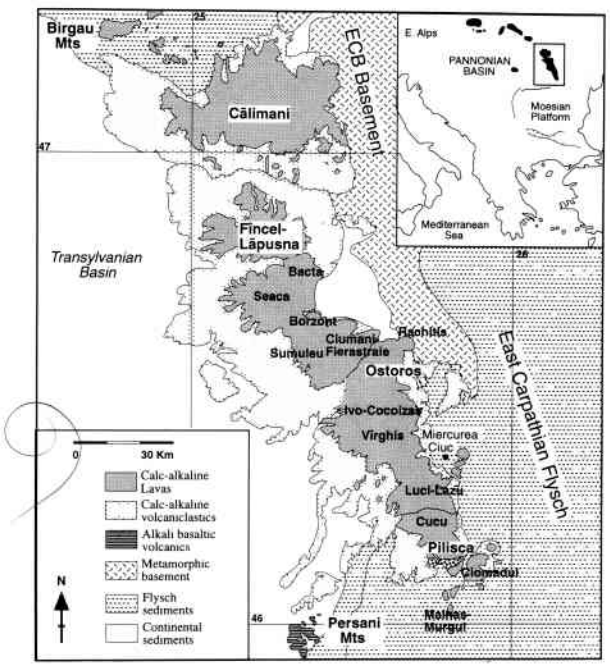

Fig. 1 – Map of the CGH volcanic province after 1:100.000 geological map of Romania (1966; 1990), showing main volcanic centers. Volcanic centres are grouped into arc segments as follows: Călimani=Călimani; Gurghiu= Fîncel-Lăpusna, Bacta, Seaca, Borzont, Sumuleu, Ciumani-Fierăstrae; Northern Harghita= Ostoros, Răchitis, Ivo-Cocoizas, Vîrghis, Sumuleu Ciuc; Southern Harghita= Luci-Lazu, Cucu, Pilisca, Ciomadul, Malnas, Murgul Mic. Inset shows the location of the CGH arc within the Carpatho-Pannonian region.

*. Present Address: NERC ICP-MS Facility, Centre for Analytical Research in the Environment, Imperial College, Silwood Park, Ascot, Berkshire, SL5 7TE, United Kingdom.

2. Local geological features

The local upper crust (Fig. 1) consists of extremely heterogeneous Precambrian to Cambrian and Mesozoic metamorphic rocks (East Carpathian Block) of low, intermediate and high grade (Burchfiel, 1976; Balintoni et al., 1989). Total crustal thickness beneath the Gurghiu and Northern Harghita Mountains is approximately 30km but thickens slightly to 40km to the north beneath the eastern Călimani Mountains and to 40km in the south beneath the Southern Harghita Mountains (Socolescu et al., 1964; Stănică et al., 1990).

To the east of the CGH arc is the East Carpathian Flysch Belt which consists of strongly folded and thrusted terrigenous sedimentary sequences (Roure et al., 1993). This represents the paleo-accretionary wedge of the Carpathian subduction zone. Volcanic rocks overlie the flysch belt in the extreme south of the CGH arc in the Southern Harghita Mountains.

Călimani is the largest volcanic centre (60 by 30km) and consists of a complex series of lavas, volcaniclastics and intrusions. Volcanism has been divided into four main stages (Seghedi, 1987) and covers a wide range of lithologies and volcanological features. The remainder of the volcanic centres are smaller and typically capped by a crater or caldera. Central volcanic edifices are dominated by lavas with more distal sequences of volcaniclastics. A detailed discussion of the volcanic features of the CGH arc is given by Szakács & Seghedi (1995).

3. Analytical techniques

Electron microprobe analyses (Tab. 1) were carried out at Birkbeck College using a JEOL-733 Superprobe equipped with a LINK systems EDS and using a 15kV accelerating potential for 100 seconds. Whole rock major and trace element concentrations (Tab. 2) were determined by XRF analysis on an automated Philips PW1400 spectrometer at Royal Holloway College. Major element oxides were measured on fused glass beads and trace elements on pressed powder pellets. Matrix corrections were calculated from major element compositions. Analytical reproducibility for most trace elements is $\sim\pm$1ppm (2 s.d.) or $\pm$1% whichever is more significant, but is approximately $\pm$0.3ppm for Nb, Rb and Y.

4. Petrography and mineral chemistry

Lithologies vary from basalt to rhyodacite with a predominance of andesitic compositions. The majority of lavas are porphyritic with fine-grained or glassy groundmasses and frequently show glomerophyric clinopyroxenes. Plagioclase is the most common crystallising phase and occurs in all lithologies. Olivine is rare but is present in some more basic rocks and a few mixed magmas. Augite and hypersthene are common pyroxenes in basaltic andesites and andesites. Hornblende crystallises in rocks with >59 wt% SiO_2 and occurs in some more basaltic compositions due to more hydrous conditions or magma mixing processes where it has reacted strongly with the groundmass. Opaque oxides range from magnetite to titanomagnetite, often coexisting with ilmenite. Most minerals are normally zoned but show strongly variable zoning profiles which may record periods of replenishment and fractionation within magma chambers.

Cognate xenoliths are widespread and are typically rich in mafic phases such as orthopyroxene $\pm$ clinopyroxene with amphibole in more evolved lithologies. Plagioclase and opaque oxides also occur. These are likely to represent fractionating phases from calc-alkaline magmas. Crustal xenoliths and xenocrysts are common on a microscopic scale. Quartz xenocrysts with strongly embayed or reacted margins are frequently seen and occasional xenoliths of gneiss, shale and quartzite are encountered. Mixing between magmas is indicated by small blebs of xenocrysts with slightly different compositions and textures that have commonly reacted with the groundmass.

Feldspar

Plagioclase (Fig. 2) varies from bytownite to oligoclase in composition (An_{23-90}) with more anorthite-rich types in more basaltic rocks. Composition may vary considerably within a single phenocryst in oscillatory-zoned bands; however, phenocryst cores are commonly quite homogeneous. Sieve textured cores are seen in many lithologies but not in all phenocrysts within a single sample, suggesting multistage crystallisation. Phenocryst rims, which are typically more sodic, are usually in equilibrium with the groundmass plagioclase composition. Inclusions of glass, opaques and microphenocrysts of pyroxene are sometimes found within plagioclases.

Alkali feldspar occurs in the groundmass of rocks from Ciomadul in the south of the CGH arc and in the shoshonitic lava domes at Malnas and Murgul Mic, some of which contain rare alkali feldspar phenocrysts. Compositions lie in the range anorthoclase-sanidine.

Pyroxene

Augite is the most common clinopyroxene found in CGH volcanics with diopside in some lithologies, particularly the high-K to shoshonitic lavas from Malnas and Murgul Mic (Fig. 3). Compositions from endiopside to

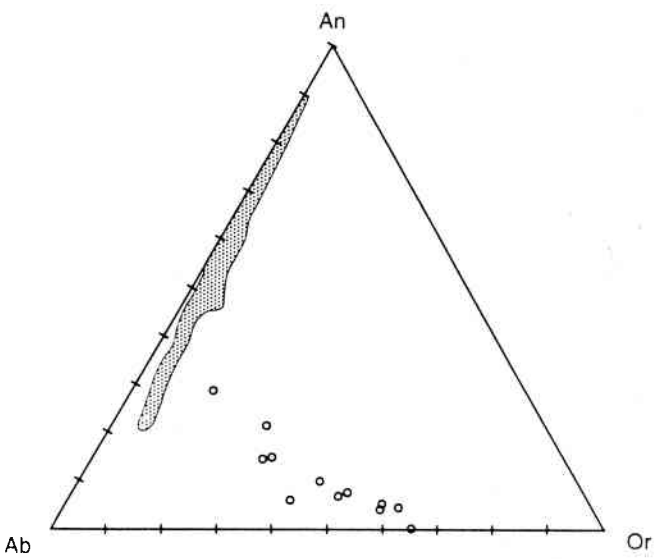

Fig. 2 – Feldspar compositions in CGH province magmas.

Table 1 – Microprobe analyses (in wt. %) of dominant phenocryst mineral phases in CGH province volcanic rocks. All samples were determined by EDS analysis at Birkbeck College.

Plagioclase

	C1	C4	C5	C7	C8	C9	G1	G3
SiO_2	53.40	49.73	54.12	52.69	54.17	56.63	49.95	51.17
Al_2O_3	28.85	31.33	28.41	29.77	29.28	27.30	31.15	30.66
FeO	0.58	0.79	0.54	0.32	0.29	0.30	0.60	0.71
CaO	12.16	15.05	11.66	12.99	11.90	9.87	14.80	14.04
K_2O	0.49	0.14	0.37	0.14	0.12	0.43	0.20	0.26
Na_2O	4.15	2.72	4.51	4.04	4.48	5.30	3.00	3.31
Total	99.63	99.76	99.61	99.95	100.34	99.83	99.70	100.15

	G7	G11	G32	H1	H2	H4	H5	H6
SiO_2	53.10	55.29	49.77	56.50	57.22	54.27	60.29	60.78
Al_2O_3	29.85	28.03	32.45	26.50	26.65	28.78	25.17	24.87
FeO	0.35	0.28	0	0.81	0.51	0.35	0	0
CaO	12.85	10.80	15.52	9.40	9.16	11.42	6.96	6.53
K_2O	2.35	0.41	0.11	1.06	0.58	0.33	0.58	0.59
Na_2O	1.95	4.97	2.50	5.17	5.66	4.65	6.67	7 03
Total	100.45	99.78	100.35	99.44	99.78	99 80	99.67	99 80

	H7	H8	H9	H13	H18	H20	H25
SiO_2	57.09	53.78	53.77	54.44	54.86	56.47	51.42
Al_2O_3	27.12	29.34	29.09	28.54	28.45	27.53	30.90
FeO	0.32	0.13	0.42	0.24	0.27	0.27	0.28
CaO	9.29	12.14	12.08	11.41	11.34	10.13	14.10
K_2O	0.42	0.24	0.68	0.33	0.29	0.43	0.13
Na_2O	5.63	4.32	3 98	4.70	4.64	5.37	3.32
Total	99.87	99.95	100.02	99.66	99 85	100.20	100.15

K-Feldspar

	H2	H3	H7	H10
SiO_2	66.82	64 23	71.07	79 91
Al_2O_3	19.29	20.02	15.71	12.68
FeO	0.54	0 48	0.55	0 27
CaO	1.93	1 73	0 03	0.64
K_2O	5 93	8 37	9 23	3.43
Na_2O	4 80	4.38	3 30	3 01
Total	99 31	99 21	99.89	99 93

Clinopyroxene

	C1	C4	C5	C9	G1	G3	G11	G32
SiO_2	51.17	50.94	51.71	52.69	53.07	51.06	52.50	52.13
TiO_2	0.98	0.96	0.48	0.42	0.53	1.09	0.30	0.85
Al_2O_3	3.35	3.43	2.00	2.37	2.34	3.82	0.97	2.61
FeO	8.19	8.84	10.14	7.04	5.81	8.74	11.13	8.14
MnO	0.20	0.22	0.35	0.23	0.13	0.23	0.30	0.19
Cr_2O_3	0.28	0.07	0.10	0.26	0.08	0.07	0	0.15
CaO	19.24	20.41	20.61	20.50	19.72	19.88	20 80	20.10
MgO	15.65	14.57	14.01	15.94	17.59	14.71	13.63	15 72
Na_2O	0.77	0.44	0.51	0.53	0.48	0.43	0 50	0.52
Total	99.83	99.88	99.91	99.98	99.75	100.03	100 13	100.41

	H1i	H1ii	H2	H3i	H3ii	H4	H8	H9
SiO_2	53.88	52.45	54.21	54.36	52.88	52.61	53 01	52.69
TiO_2	0.38	0.39	0.45	0.32	0.66	0.50	0	0.27
Al_2O_3	1.54	2.26	1.76	1.27	1.86	1 77	0.79	1.06
FeO	3.19	7.65	3.65	2.89	6.76	8.82	11.86	11.50
MnO	0	0.24	0.11	0	0.24	0 26	0.24	0.38
Cr_2O_3	0.53	0	0.50	0.74	0	0.05	0	0
CaO	22.12	22.95	21.52	22.46	21.36	20.65	21.37	20.62
MgO	17.45	13.34	17.43	17.65	15.65	14.84	12.63	13.27
Na_2O	0.41	0.61	0.45	0.48	0.54	0.48	0.41	0.44
Total	99.50	99.89	100.08	100.17	99.95	99.98	100.31	100.23

	H13	H11
SiO_2	50.79	52.78
TiO_2	0.86	0.48
Al_2O_3	4.12	3.74
FeO	6.61	3.26
MnO	0 17	0.18
Cr_2O_3	0.12	0.64
CaO	21.60	20.80
MgO	15.23	17.08
Na_2O	0.33	0.84
Total	99.83	99.80

Orthopyroxene

	C4	C5	C7	C9	G3	G7	G11	G32
SiO_2	52.58	54.01	55.31	54.92	53.12	52.01	51.70	53.00
TiO_2	0.61	0.29	0	0.20	0	0.15	0.11	0.22
Al_2O_3	1.43	1.13	2.10	2.06	0.40	0.44	0.49	0.58
FeO	16.85	17.02	10.57	12.03	26.65	27.73	29.46	24.28
MnO	0.57	0.53	0.31	0.29	0.69	0.64	0.94	0.48
Cr_2O_3	0	0	0.55	0.37	0	0	0	0
CaO	8.78	1.20	1.15	1.29	1.13	1.13	1.03	1.26
MgO	18.49	25.54	29.89	28.64	17.86	17.79	16.39	20.12
Na_2O	0.43	0	0	0.20	0	0	0	0.23
Total	99.74	99.72	99.88	100.00	99.85	99.89	100.12	100.17

	H1	H3	H4	H8	H9	H13	H18
SiO_2	52.82	54.71	52.77	52.26	52.88	51.98	52.38
TiO_2	0.13	0.36	0.17	0.08	0.14	0.12	0.14
Al_2O_3	0.37	0.96	1.14	0.40	0.68	0.58	0.52
FeO	24.09	15.56	22.28	27.22	23.86	26.34	27.13
MnO	0.42	0.54	0.60	0.67	0.59	0.81	0.62
Cr_2O_3	0	0	0	0	0	0	0
CaO	1.88	1.93	1.19	1.13	1.36	0.80	1.09
MgO	20.10	26.16	21.54	18.02	20.61	19.05	18.17
Na_2O	0.13	0.21	0	0.13	0	0.22	0.20
Total	99.94	100.43	99.69	99.91	100.12	99.90	100.25

Amphibole

	C7	C8	C9	H4	H5	H6	H7	H8
SiO_2	44.68	42.47	45.80	48.88	45.69	48.17	42.37	44.98
TiO_2	1.70	1.51	1.87	1.22	1.71	1.02	2.18	2.42
Al_2O_3	10.87	14.47	11.57	11.93	9.86	7.62	12.30	9.43
FeO	15.13	11.89	7.94	10.29	11.40	11.53	13.12	15.36
MnO	0.41	0.21	0.25	0	0.16	0.26	0.11	0.14
Cr_2O_3	0	0	0.16	0	0	0.04	0.04	0.02
CaO	10.35	11.12	10.85	10.03	11.74	11.68	11.68	10.94
MgO	12.35	13.75	16.65	12.15	14.68	15.10	12.70	11.95
K_2O	0.22	0.21	0.22	0.39	0.87	0.75	1.02	0.69
Na_2O	1.90	2.55	2.89	3.02	1.90	1 76	2.32	1.90
Total	97.61	98.18	98.20	97.91	98.01	97 93	97.84	97.83

Biotite

	H3	H4	H5	H6	H7
SiO_2	40.00	42.97	37.38	37.59	37.39
TiO_2	5.87	2.33	4.31	3.86	4.62
Al_2O_3	13.31	13.29	14.21	13.91	14.78
FeO	7.42	10.54	17.45	16.19	15.19
MnO	0.02	0	0	0.04	0
MgO	19.97	17.56	13.45	14.07	14.64
K_2O	8.67	8.02	8.91	8.95	8.81
Na_2O	0.90	0.53	0.72	0.57	0.90
Total	96.16	95.24	96.43	95.18	96.33

(a) Feldspar compositions, (b) Clinopyroxene compositions. Two populations are shown for samples H1 and H3, (c) Orthopyroxene compositions, (d) Amphibole and Biotite compositions.

Table 2 – Selected major and trace element data for ECV rocks determined by XRF analysis and calculated on a volatile-free basis. Major elements are given in Wt% and trace elements in ppm. Standard errors and reproducibility are reported in the text. Analyses marked * are from Mason et al., in press.

	Călimani -Pre-Caldera group						*Fîncel-Lăpusna*					
	C6*	C36	C64	C37	C29	C27	G17	G11	G12*	G14	G18	G27
SiO_2	53.94	55.15	55.33	56.96	59.31	60.47	52.54	54.41	54.97	58.71	59.53	61.47
Al_2O_3	16.85	17.46	17.86	18.30	18.80	18.42	19.21	19.05	18.70	18.09	18.26	17.60
Fe_2O_3	9.46	8.40	8.36	7.40	6.47	5.74	8.85	8.18	8.70	7.07	6.42	6.11
MgO	4.42	4.18	4.25	3.69	2.42	2.22	5.07	3.94	4.23	3.33	3.28	1.91
CaO	8.35	8.41	8.15	7.52	6.75	6.12	9.03	8.69	8.31	7.19	7.16	5.79
Na_2O	3.10	2.83	3.15	3.27	3.46	3.30	3.19	3.18	2.96	3.27	3.25	3.84
K_2O	1.887	1.831	1.379	1.742	1.709	2.38	0.990	1.037	1.166	1.274	1.175	1.850
TiO_2	0.993	0.931	0.923	0.806	0.618	0.614	1.011	0.981	0.967	0.780	0.678	0.721
MnO	0.176	0.170	0.137	0.183	0.121	0.131	0.177	0.129	0.166	0.115	0.142	0.104
P_2O_5	0.326	0.216	0.180	0.186	0.181	0.164	0.181	0.123	0.145	0.169	0.169	0.193
Total	99.50	99.58	99.72	100.06	99.85	99.55	100.25	99.72	100.32	99.99	100.05	99.59
Mg#	0.48	0.50	0.50	0.50	0.43	0.43	0.531	0.488	0.491	0.483	0.503	0.382
LOI	2.18	0.80	0.73	1.31	1.18	1.15	1.49	0.51	0.28	0.65	4.47	2.66
Ni	27	22	14	12	7	6	21	11	8	15	15	10
Cr	32	52	37	25	14	4	27	25	17	43	31	17
V	235	205	215	155	103	103	236	256	248	153	141	130
Sc	27	31	29	22	13	14	30	32	31	22	20	16
Cu	74	40	53	21	19	34	29	20	23	27	36	23
Zn	86	80	73	75	75	76	69	72	82	75	78	76
Ga	20	18	18	20	18	19	20	19	19	18	18	18
Pb	9.9	8.7	11.8	8.0	9.5	14.2	2.6	7.7	9.6	6.9	5.8	9.3
Sr	481	368	250	318	314	270	263	256	282	280	244	271
Rb	52.2	55.8	52.0	59.9	61.1	79.3	27.5	33.0	36.9	45.4	35.9	62.5
Ba	442	394	332	332	315	372	237	200	207	257	309	451
Zr	112	164	132	161	150	165	124	97	104	145	147	174
Nb	8.0	9.6	6.5	8.8	7.9	8.7	6.0	5.5	6.6	7.8	8.3	11.5
Th	4.0	5.3	5.0	5.5	4.8	6.4	2.2	2.8	3.0	4.8	4.5	11.3
Y	24.0	32.3	26.1	24.6	22.1	25.5	24.9	24.8	25.4	26.5	21.7	22.9
La	21	22	14	21	17	19	10	11	13	18	14	22
Ce	44	46	29	43	36	39	24	23	28	33	30	41
Nd	24	23	16	21	18	18	14	14	15	17	14	20

	Fîncel-Lăpusna low K-series				*Ostoros*				*Pilisca*			
	G21	G20	G13	G25	H31	H30	H43	H44	H4*	H12*	H47	H50
SiO_2	56.06	59.73	62.30	63.31	60.82	60.94	62.21	67.75	59.46	63.16	64.72	66.53
Al_2O_3	18.81	18.96	17.88	17.58	17.22	17.62	17.54	16.99	17.69	17.51	17.31	17.46
Fe_2O_3	8.04	6.64	5.56	5.35	5.86	5.76	5.14	4.04	5.14	4.27	3.96	3.75
MgO	3.54	2.16	2.29	1.88	3.59	3.07	2.40	0.10	3.57	2.18	1.67	1.29
CaO	8.31	6.98	6.18	6.04	6.46	6.24	5.91	3.72	5.98	4.92	4.51	4.09
Na_2O	3.17	3.88	3.62	3.90	3.26	3.23	3.43	4.52	4.01	4.38	4.03	3.91
K_2O	0.490	0.963	1.004	1.230	2.038	2.074	2.139	2.643	2.166	2.581	2.540	2.624
TiO_2	0.737	0.621	0.568	0.590	0.652	0.641	0.515	0.441	0.795	0.586	0.559	0.516
MnO	0.160	0.184	0.118	0.109	0.128	0.120	0.124	0.029	0.090	0.101	0.095	0.074
P_2O_5	0.225	0.202	0.165	0.161	0.119	0.127	0.145	0.168	0.172	0.197	0.140	0.134
Total	99.55	100.32	99.69	100.15	100.14	99.83	99.54	100.39	99.07	99.88	99.54	100.38
Mg#	0.47	0.39	0.450	0.410	0.548	0.514	0.481	0.045	0.579	0.503	0.456	0.406
LOI	0.32	1.15	0.69	0.61	0.59	0.48	1.58	1.03	0.69	1.35	0.81	1.39
Ni	17	6	10	10	17	6	8	4	18	7	9	7
Cr	45	7	20	22	68	19	13	4	53	13	18	12
V	151	90	101	98	107	106	102	26	134	81	52	59
Sc	22	12	14	14	17	16	15	5	18	11	10	9
Cu	34	25	18	12	14	8	18	6	18	7	5	4
Zn	80	89	60	57	62	65	75	65	49	41	46	47
Ga	18	18	17	18	17	18	16	17	19	18	17	17
Pb	3.2	5.2	6.2	6.0	7.5	8.3	9.1	12.2	22.0	15.6	13.7	15.4
Sr	510	272	300	267	309	374	314	305	1181	871	529	503
Rb	15.3	30.3	27.6	50.0	74.2	75.5	76.3	95.2	53.2	70.2	86.7	93.4
Ba	87	208	213	199	392	409	410	502	876	1128	771	743
Zr	106	155	142	143	135	149	150	204	125	124	139	139
Nb	4.0	7.5	7.0	6.7	8.0	8.3	7.1	9.2	14.4	20.3	16.6	16.6
Th	1.1	3.3	3.4	4.0	8.6	9.0	8.6	11.0	8.2	13.3	11.5	11.5
Y	22.5	22.9	20.1	18.4	18.6	20.9	18.1	18.2	17.5	15.7	17.0	23.2
La	10	13	14	13	19	24	21	27	28	38	29	32
Ce	25	29	30	26	35	41	39	49	50	64	51	55
Nd	17	15	15	14	14	18	15	20	22	23	18	21

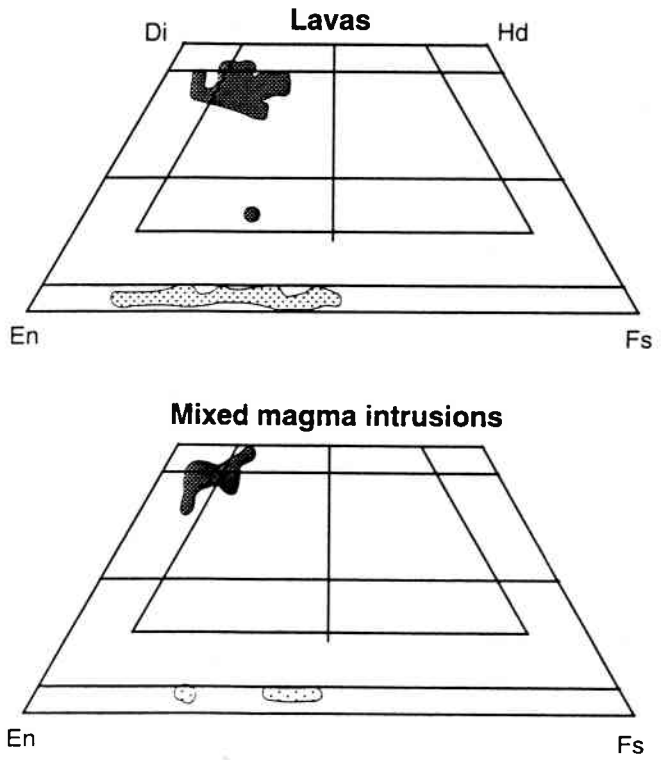

Fig. 3 – Pyroxene compositions in CGH magmas for (a) lavas and intrusions from the major volcanic centres; and (b) high-K to shoshonitic mixed magma intrusions of Malnas and Murgul Mic.

titanaugite are also found. Such a wide variation in composition within individual rocks indicates crystallisation over a wide range of temperatures (Lindsley, 1983; Matthews et al., 1994). Both normal and reverse zoning is seen within phenocrysts but variations in composition are much less pronounced than in the plagioclases. Clinopyroxene is frequently glomerophyric and small opaque inclusions, commonly magnetite, are very common. A few xenocrysts of sub-calcic augite were identified in a basaltic andesite from Călimani (Fig. 3).

Orthopyroxene compositions vary from 50 to 90% enstatite (Fig. 3). Euhedral phenocrysts are typically smaller than clinopyroxene within the same sample. Opaque inclusions are rare. The proportion of orthopyroxene to clinopyroxene varies considerably between lithologies; however, orthopyroxene is more common in andesitic rocks. Zoning may be normal or reverse with phenocryst rims having similar compositions to microphenocrysts in the groundmass.

Geothermometry has been carried out on clinopyroxene-orthopyroxene pairs using the techniques of Wells (1977) and Wood & Banno (1973). Temperatures were estimated from mean mineral analyses; however, care was taken to ensure that a representative population was used, especially where more than one population of pyroxene may have resulted from magma mixing. The composition of phenocryst rims and groundmass microphenocrysts were used to estimate the magmatic temperature at the time of crystallisation. Calculated temperatures lie in the range 1150-860°C for basaltic to dacitic magmas with more parental, mafic magmas generally 200°C hotter than evolved silicic magmas (Fig. 4).

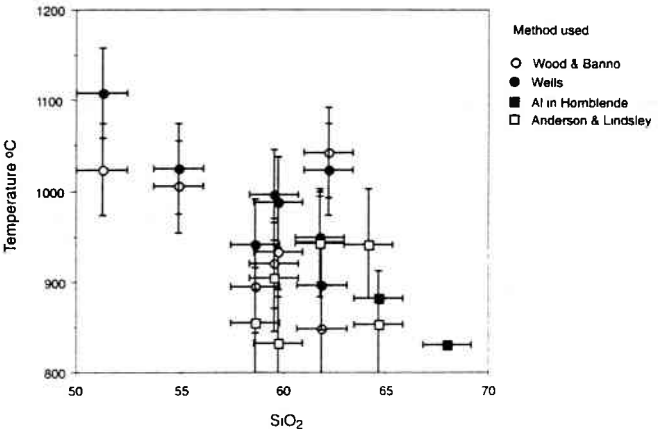

Fig. 4 – Variation of magmatic temperature with melt composition. Two pyroxene geothermometers are calculated using the methods of Wells (1977) and Wood & Banno (1973). Geothermometers using magnetiteilmenite pairs (Andersen & Lindsley, 1988) and the Al-in-Hornblende method (Blundy & Holland, 1990) are also shown.

Amphibole

Hornblende is a ubiquitous phenocryst in more evolved lithologies. Margins are typically rimmed with opacite (opaque-rich aggregates) and may be corroded or ragged. In some cases, phenocrysts have been wholly replaced by opacite or by a fine-grained mass of plagioclase, opaques and pyroxenes.

Hornblende analyses have been used to estimate magma chamber pressures and temperatures using the Al-in-hornblende system (Johnson & Rutherford, 1989; Blundy & Holland, 1990) in magmas from Ciomadul, Malnas and Murgul Mic where alkali feldspar is an equilibrium phase. Pressure estimates for these volcanic centres are in the range 2.82-5.55kb suggesting upper to mid-crustal depths of approximately 10-20km. Temperatures given by this model are in the range 830-882°C (Fig. 4).

Opaque oxides

Magnetite, titanomagnetite and ilmenite occur in all lithologies and are ubiquitous as groundmass phases or microphenocrysts. Large phenocrysts are rare. Both titanomagnetite or magnetite (less common) and ilmenite commonly coexist. In some phenocrysts, exsolution lamellae of one oxide occur in the other, indicating slow cooling and oxidation. Magnetite inclusions are frequently found enclosed in clinopyroxene phenocrysts.

Geothermometry using ulvöspinel and ilmenite activities (Andersen & Lindsley, 1988) gives temperatures in the range 832-947°C. Agreements with temperatures determined by two-pyroxene and the Al-in-Hornblende methods are within analytical error in most cases (Fig. 4).

Others

Olivine in CGH rocks has a wide variation of compositions from Fo_{52} to Fo_{90}. Many basaltic rocks contain oli-

vine but it is frequently altered to serpentine. Only samples with fresh olivine have been analysed and included in this study. The most Fo-rich olivine occurs in the Malnas and Murgul centres which is much more Mg-rich than in the remainder of the basaltic samples.

Biotite is found in high-K lavas and intrusions at the southern end of the CGH arc. It commonly contains inclusions of zircon which are surrounded by pleochroic haloes. Biotite has also crystallised alongside plagioclase, quartz and Fe-Ti oxides in early rhyodacitic melts from Călimani. Sphene is a phenocryst phase in a few lavas from Ciomadul and is also found in Malnas and Murgul Mic. It is euhedral and has a uniform composition. Almandine garnet occurs in a few intrusions from Călimani and has been recorded in a high-K biotite-bearing intrusion on the eastern flanks of Vîrghis where it appears to be in equilibrium with the groundmass. Apatite is rich in rocks from Cucu and Ciomadul and is common as small inclusions, particularly in plagioclase, in rocks from other centres.

5. Bulk rock chemical composition

Most CGH volcanic centres are medium-K calc-alkaline (Fig. 5) and show tightly defined trends on a SiO_2 vs. K_2O plot with minor internal variation (Mason et al., in press). SiO_2 contents vary from 51 to 71 wt%. The majority of volcanic centres overlap in composition and appear to diverge from a common parental end-member. However, the large Călimani complex covers a wider range in compositions, including a low-K and a higher-K series. Fîncel-Lăpusna (in the Gurghiu segment) contains four samples which form a low-K series, reaching almost tholeiitic compositions. In the extreme south of the arc, volcanic centres are high-K calc-alkaline. In centres from Cucu southwards, average K_2O progressively increases until slightly shoshonitic compositions are reached in Malnas and Murgul Mic (Seghedi et al., 1986, 1987).

Major element Harker diagrams are presented here for representative volcanic centres (Fig. 6). CaO, Fe_2O_3 and TiO_2 are strongly compatible within the centres and small variations are seen between the centres. Some scatter is seen within the data involving MgO, Al_2O_3 and MnO. Na_2O is very scattered and P_2O_5 shows little variation but concentrations of P_2O_5 decrease between certain samples.

The highest concentrations of Ni and Cr are found within andesitic lithologies rather than in more basic compositions (Fig. 6). However Sc, V and Y are strongly compatible and show clear negative variations with SiO_2 content. Y commonly behaves slightly incompatibly or slightly compatibly until around 59% SiO_2 when it becomes more strongly compatible. Pb, Rb and Th are broadly incompatible but show some scatter and Sr is also scattered.

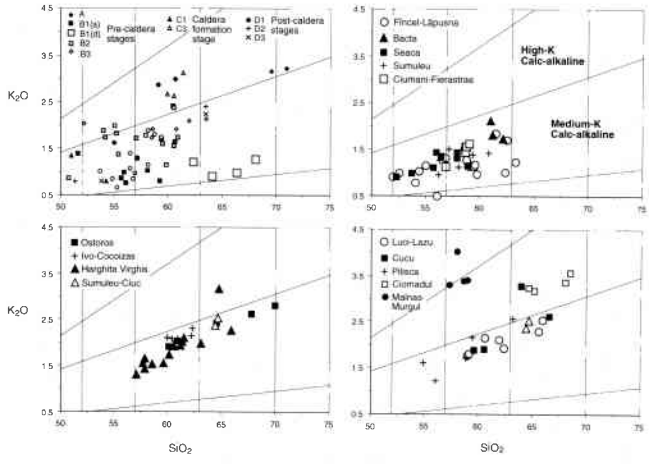

Fig. 5 – K_2O vs. SiO_2 in CGH province magmatic rocks (a) for the Călimani volcanic centre, (b) for centres from the Gurghiu Mountains, (c) for Northern Harghita are volcanic edifices and (d) for the Southern Harghita Mountains arc segment.

6. Processes affecting magma composition

The Călimani volcanic complex contains a wide range of lithologies and has a complex structure (Seghedi, 1987). Magmas probably evolved from more than one magma chamber over the period of approximately 2.5Ma during which Călimani was active. Thus, rocks produced at the beginning of the eruptive cycle could have undergone a different evolution to those which crystallised at the end. The complex nature of Călimani precludes a detailed discussion of fractional crystallisation for much of the centre; however, fractionation can be investigated within small magma series which are closely related both in the field and in chemistry. Most major elements show well-defined linear trends with fractionation indices such as SiO_2, but there is significant scatter shown by some elements, particularly Al_2O_3. MgO, MnO and P_2O_5 concentrations are also scattered, some of which could be caused by fractionation in separate magma plumbing systems during different periods of magmatic evolution.

A «pre-caldera» eruptive series (Fig. 6) has been selected in which to investigate fractional crystallisation. Al_2O_3 is incompatible within the andesitic samples, suggesting that plagioclase did not fractionate. Small amounts of plagioclase removal may have started as the melt reached 59-60% SiO_2. Basalts of the series are high in Al_2O_3 and do not correspond to the low Al_2O_3 fractionation scheme in the andesites. Heterogeneous accumulation of plagioclase was probably responsible for the wide variation in Al_2O_3. Na_2O behaved incompatibly supporting the lack of plagioclase fractionation or suggesting the removal of only basic plagioclase.

In the remainder of the CGH arc, volcanic centres are smaller and more easily resolved by field relationships. Magmas are likely to have evolved from more simple magma plumbing systems. This is reflected in more closely defined trends on Harker diagrams. In Gurghiu, rocks from the Fîncel-Lăpusna volcanic edifice (Fig. 6) show good evidence for fractional crystallisation involving plagioclase, the pyroxenes and Fe-Ti oxides. However, some scatter is seen in Al_2O_3 and MnO when plotted against SiO_2. Anomalously high concentrations of Al_2O_3 could be due to plagioclase accumulation in some lavas, which is confirmed by the plagioclase-rich nature of these rocks in thin-section. P_2O_5 and Y are also high within two of the plagioclase-rich samples suggesting the additional accumulation of apatite. Amphibole removal occurred only in the most evolved magmas, where Y was removed. Four samples appear to form a low-K series which may have undergone evolution in a separate magma chamber. These rocks are also lower in Pb, Rb and Th.

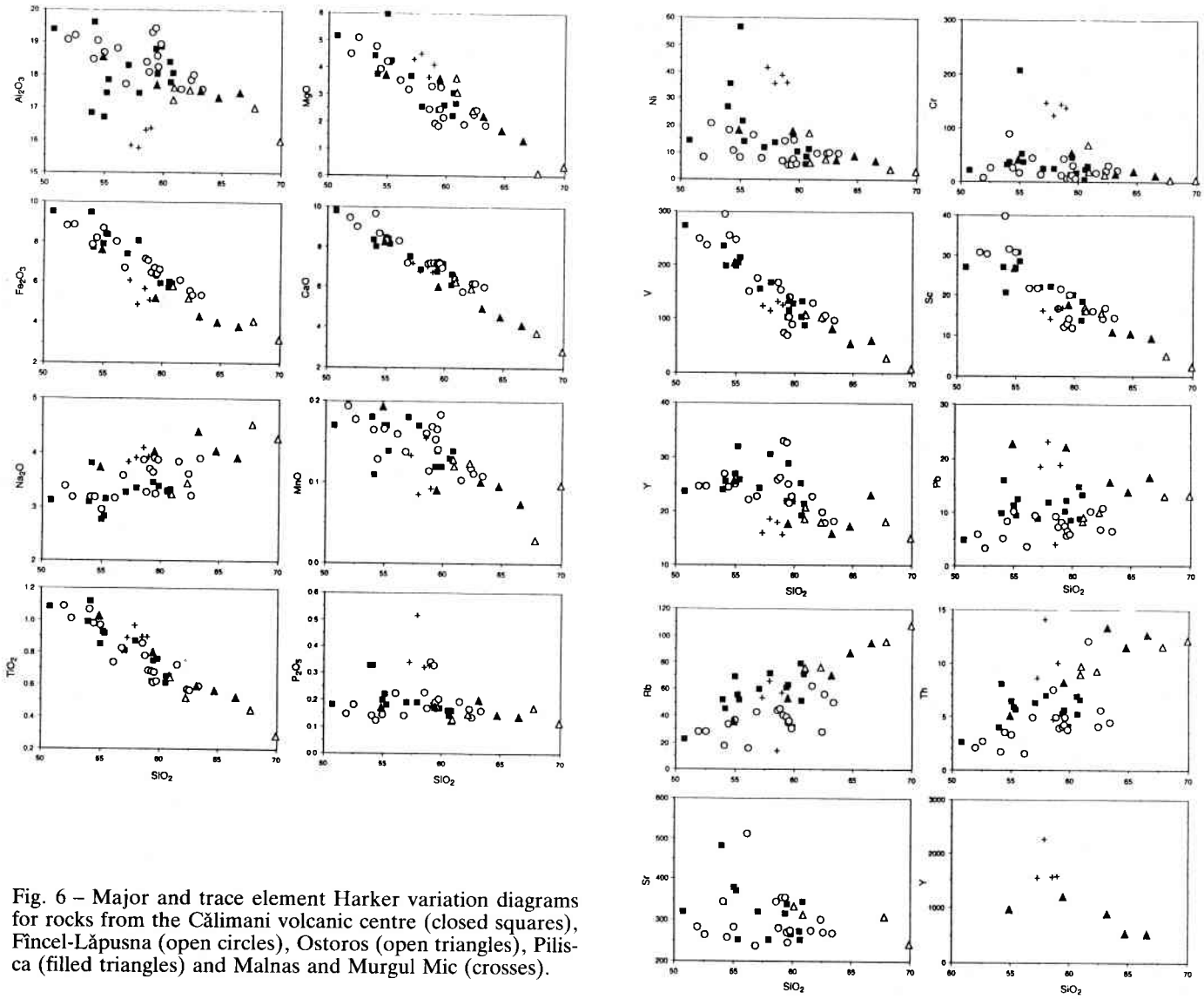

Fig. 6 – Major and trace element Harker variation diagrams for rocks from the Călimani volcanic centre (closed squares), Fîncel-Lăpusna (open circles), Ostoros (open triangles), Pilisca (filled triangles) and Malnas and Murgul Mic (crosses).

Scatter within the data is seen in other volcanic centres from Gurghiu and can be explained by similar phenocryst accumulation processes. Major and trace elements vary more consistently with fractionation in the Northern Harghita arc segment, but some scatter is observed, also caused by variable fractionation and accumulation. Fractionation systems in Fîncel-Lăpusna are a good model for most of these volcanic centres.

In the Southern Harghita magmas, fractionation processes varied quite considerably between volcanic centres. Luci-Lazu behaved in a similar manner to more northerly centres in the Northern Harghita area and appeared to have fractionated plagioclase, pyroxenes, Fe-Ti oxides and apatite. However, Pilisca and Ciomadul crystallised predominantly amphibole and biotite alongside plagioclase and the fractionation of these phases had more control over magma chemistry. Trends for Pilisca are closely correlated (Fig. 6) except for some incompatible elements (e.g. Pb) and this is typical for all of the centres in this area.

Rocks from the Malnas and Murgul Mic high-K to shoshonitic lava domes have slightly anomalous chemistries. Samples plot close together on all the Harker diagrams (Fig. 6) and are distinctively high in MgO, P_2O_5, TiO_2, Ni, Cr, Sr and Pb. Al_2O_3, Fe_2O_3 and Y are low. These slight differences in chemistry occur in combination with the unusual mineralogies.

When the effects of phenocryst accumulation are removed and rocks are grouped into suites of similar age and location, approximately linear trends are seen on Harker diagrams within all of the volcanic centres, suggesting that fractional crystallisation was a dominant petrogenetic process. This assertion is supported by the common occurrence of cognate xenoliths in CGH rocks. Minerals which have been suggested as fractionating phases are all found as cognate material.

Least-squares fractional crystallisation modelling (Wright & Doherty, 1970) has been carried out using mean analyses of phenocrysts from the more parental magmas and analyses of mineral phases in cognate xenoliths (Tab. 3). For the complex Călimani centre there may be some disparity between the selected mineral analyses and the minerals in parental magmas. Numerical methods support qualitative observations of the fractionation of plagioclase, orthopyroxene, clinopyroxene, magnetite, ilmenite and apatite. Amphibole fractionated in more evolved lithologies and was important in only a few volcanic centres. Biotite was a fractionating phase in only Pilisca (Tab. 3) and Ciomadul. Residuals vary within each centre from relatively low to quite high

Table 3 – Least squares fractional crystallisation models on rock pairs from CGH volcanic centres. F is the amount of melt remaining and R^2 is the sum of the squares of the residuals.

Călimani- Pre-Caldera group

Pairs	F	Plag	Opx	Cpx	Mt	Ilm	Ap	R^2
C6-C36	0.97		1.22		1.34	0.13	0.47	0.2153
C36-C37	0.93			4.44	1.14	0.31	0.81	0.3795
C36-C64	0.98			1.28	0.06	0.02	0.23	0.3908
C29-C27	0.93	4.91	0.45	1.00	0.90			0.3820

Fîncel-Lăpusna

Pairs	F	Plag	Opx	Cpx	Mt	Ilm	Ap	R^2
G17-G11	0.82	9.98	5.65		1.49	0.25	0.23	0.2138
G11-G12	0.96	3.58				0.10	0.22	0.1779
G14-G18	0.97	1.08	0.45	0.07	0.72	0.20	0.12	0.0364
G18-G27	0.83	10.24	4.19	2.25		0.34		0.3543

Fîncel-Lăpusna low-K series

Pairs	F	Plag	Opx	Cpx	Amph	Mt	Ilm	R^2
G21-G20	0.80	10.85	4.47	2.17	1.53	0.51	0.75	0.5301
G20-G13	0.89	8.83	0.04		1.69	0.03	0.07	0.3027
G13-G25	0.93	4.72	2.21		0.19	0.03		0.0755

Ostoros

Pairs	F	Plag	Opx	Cpx	Amph	Mt	Ilm	R^2
H31-H43	0.90	3.03	2.73	1.87	1.39	0.49	0.15	0.0318
H30-H43	0.93	3.92	2.52	0.27		0.60	0.21	0.0119
H43-H44	0.76	8.77	1.56	1.46	12.22	0.58	0.45	0.7547

Pilisca

Pairs	F	Plag	Amph	Bi	Mt	Ilm	Ap	R^2
H4-H12	0.80	6.74	8.87	3.85		0.32	0.33	0.2707
H12-H47	0.92	2.96	2.05	2.29	0.19	0.06	0.24	0.2936
H47-H50	0.94	1.80	3.56	0.34	0.01	0.11	0.14	0.0720

Crustal contamination models

Pairs	F	Plag	Opx	Amph	Mt	Ilm	Ap	Crust	R^2
C2-C3	0.92	5.34		1.44	0.94	0.01			0.5759
C2-C3	0.96	5.39		1.14	1.34	0.05		-4.02	0.5381
H18-H16	0.83	15.00	2.87		0.81	0.44	0.46		0.4034
H18-H16	0.98	13.12	3.33		1.39	0.54	0.08	-16.65	0.1228

$^{87}Sr/^{86}Sr$ from Mason *et al.*, in press:
C2= 0.70416; C3= 0.70445; H18=0.70657; H16= 0.70682

values and this is reflected in the scatter seen on major and trace element Harker diagrams. The models are strongly dependant on mineral chemistry and small variations in the major element contents of some minerals can have a large effect on the modelling. However, some additional processes may have caused the high residual values. Several factors could have contributed to this scatter, most notably magma mixing, crustal assimilation and crystal accumulation.

Magma mixing between basic and acidic end-members could have produced similar trends to those predicted by fractional crystallisation on major and trace element Harker diagrams. Petrographic evidence for mixing is widespread in volcanic rocks from the CGH province. Mixing has been identified on both a hand-specimen and a microscopic scale. In hand-specimen, small blebs of magmatic material are seen enclosed within a host rock. Blebs commonly have rounded margins, a different texture to that of the host sample and contain a different mineral assemblage or minerals of a slightly different composition. Reaction with the groundmass can be seen by a preferential crystallisation of orthopyroxene around the rims. This type of mixing is particularly noticeable in the Cucu volcanics (Mason, 1995).

Xenocrysts are common in all types of lithology on a microscopic scale, but are particularly prevalent in andesites. Two populations of common mineral phases such as pyroxene may occur, with normal zoning in one population and reverse zoning in the other. Small inclusions of xenocrysts, up to a few mm across, are sometimes seen but can be difficult to distinguish from cognate xenoliths. The most spectacular example of magma mixing is seen in Malnas and Murgul Mic, high-K lava domes at the southern end of the CGH arc. Malnas contains coexisting Mg-olivine (Fo_{88-90}), quartz, two populations of clinopyroxene, two populations of orthopyroxene plus amphibole and biotite. Small amounts of sphene, zircon and apatite are also found along with a few rare phenocrysts of K-feldspar. The quartz is probably of crustal origin. The large xenocrysts are rounded and have well-defined reaction rims of orthopyroxene. Amphibole is of an unusual composition of the tremolite-actinolite series and is probably of crustal origin as a xenocryst phase. The rock appears homogeneous on a hand-specimen and field scale with no evidence for mixing. The magmas were probably erupted through crustal basement rocks at depth. Crustal source rocks are medium to high grade schists, gneisses and amphibolites but the presence or absence of this material at depth beneath the southern end of the chain cannot be proven. Such crust would be a feasible source for the amphibole and quartz. The olivine is unusually Mg-rich and is of a composition usually associated with mantle peridotites. It may have originated from disaggregated mantle xenoliths in a similar manner to that proposed for olivine xenocrysts in alkali basalts of the Persani Mountains (Downes et al., 1995).

Magma chamber replenishment is a major mechanism for mixing and this can be identified from zoning profiles of plagioclases and pyroxenes. In some rocks more than one replenishment event has taken place. The injection of basic material into a magma chamber, which may be up to 200°C hotter than the host magma, could produce a strong convective overturn which would thoroughly mix the two magmas.

The effect of magma mixing on major and trace element trends is difficult to quantify. Mixing and fractionation were likely to have occurred together and could have produced similar trends. If the two end-members are from the same magmatic system, which has been crystallising and fractionating an identical mineral assemblage, then the product will lie along the same trend as that produced by fractionation. Mixing may explain some of the high residuals predicted by least squares fractional crystallisation modelling. Scatter on Harker plots would only be produced by mixing in a suite where the fractionating mineral assemblage changes (i.e. producing a point of inflection on a Harker diagram) or where unusual magma compositions such as a crustally contaminated magma are mixed with the basic end-member.

The addition of small amounts of crustal material to CGH magmas is proven by the presence of crustal xenoliths and xenocrysts within certain lavas. However, without extensive field sampling or the study of many thin-

sections, crustal material may not always be identified in rocks which are contaminated. CGH magmas have been investigated isotopically (Mason, 1995; Mason et al., in press) and found to have been strongly contaminated in the upper crust. $^{87}Sr/^{86}Sr$ and $^{143}Nd/^{144}Nd$ extend over a wide range and can be explained by mixing parental magmas with a variety of contaminants from the local upper crust.

Magmas would have been initially hot enough to melt and assimilate upper crustal lithologies. Assimilation probably took place through partial rather than batch melting and this is supported by the dispersal of xenocryst phases throughout the contaminated magmas.

Crustal contamination can be verified by adding small amounts of crust to the least squares fractional crystallisation models. This has been attempted here for rocks from the Călimani and Luci-Lazu volcanic centres. Within each centre, rocks have been taken which are related by fractionation and variably contaminated (Mason et al., in press). Sample pairs C2 to C3 and H18 to H16 are progressively more enriched in $^{87}Sr/^{86}Sr$ with increasing SiO_2. Schist from the local crust (Mason et al., in press) can be added to the mixing calculations for steps C2 to C3 and H18 to H16. Calculated residuals are reduced by adding crust of this composition. However, residuals are often reduced by simply adding another phase to the calculation. Thus, assimilation is viable but not proven by this method. The most important point is that assimilation of crust may explain some of the high residuals in fractional crystallisation models for CGH magmas. A noticeable problem is that adding crust can affect the phases which will work in the modelling.

Phenocryst accumulation can considerably affect least squares models and produce significant scatter on major and trace element Harker diagrams. This has been demonstrated qualitatively and such samples have been omitted from the calculations. This preferential accumulation, usually of plagioclase, suggests possible tapping of the margins of a magma chamber during a more closed system evolution. A simple model of a single fractionating body is precluded.

The least squares modelling outlined above does have significant limitations and has been carried out to show that fractional crystallisation is a viable process in CGH magmas rather than trying to prove that it took place. Mineral compositions vary widely within a single sample and the compositions taken for the purposes of the modelling are clearly approximations of what may have been fractionated. Small variations in the chemistry of the mineral phases used in the modelling can have a large effect on the proportion of fractionation of that mineral and on the sum of squares of the residuals.

7. Conclusions

The CGH arc segment is a large chain of complex interrelated calc-alkaline volcanic edifices. Lavas and intrusions from each of the central structures have been investigated chemically and found to show large ranges in mineral and bulk compositions. Major crystallising phases vary between compositions which are in equilibrium with basic and acidic melts.

Fractional crystallisation controlled significant changes in major and trace element geochemistry in CGH magmas. Plagioclase, pyroxenes, amphibole, biotite, apatite and Fe-Ti oxides were all important fractionating phases to varying degrees. Orthopyroxene fractionation was typically more dominant than clinopyroxene fractionation. Amphibole crystallised and fractionated in rocks with >59% SiO_2 except in a few cases where more basic magmas were hydrated or mixed with acidic melts. Apatite fractionation was important in several, but not all, volcanic centres.

Variations in the type and proportions of fractionating minerals are seen between volcanic centres and within individual magma series. Basaltic andesites and andesites from the precaldera group from Călimani did not fractionate plagioclase. Elsewhere plagioclase was the most important fractionating phase. Biotite and amphibole replaced pyroxene as the controlling mafic phases in the Pilisca and Ciomadul volcanoes from the southern end of the arc.

Residuals calculated by least squares modelling are low to relatively high. Higher values are due to mixing with other (often closely related) magmas and assimilation of crustal material. Residuals are reduced by adding crust to the least squares fractionation models.

Acknowledgements

A. Beard is thanked for advice and assistance during electron microprobe work at Birkbeck College. We are grateful to G. Marriner and G. Ingram for assistance during analytical work at Royal Holloway, University of London. G. Dobosi and A. Peccerillo are thanked for helpful reviews. The Romanian Institute of Geology gave logistical support during fieldwork in the East Carpathians. P.M. acknowledges a postgraduate research studentship from NERC. H.D. is grateful for support from the Birkbeck College Research Fund and the University of London Central Research Fund.

REFERENCES

Andersen, D.J. & Lindsley, D.H. (1988): Internally consistent solution models for Fe-Mg-Mn-Ti oxides. Am. Mineral., 73, 714-726.

Balintoni, I., Berza, T., Hann, H.P., Iancu, V., Kräutner, H.G. & Udubasa, G. (1989): Precambrian metamorphics in the South Carpathians: Multilateral cooperation of the Academies of Sciences of the Socialist Countries, Earth crust structure evolution and metallogeny. Guide to Excursions. 89 pp.

Blundy, J.D. & Holland, T.J.B. (1990): Calcic amphibole equilibria and a new amphibole-plagioclase geothermometer. Contrib. Mineral. Petrol., 104, 208-224.

Burchfiel, B.C. (1976): Geology of Romania. Geol. Soc. Am. Spec. Publ., 158, 82 pp.

Csontos, L. (1995): Tertiary tectonic evolution of the Intra-Carpathian area: A review. In: «Neogene and related magmatism in the Carpatho-Pannonian Region», H. Downes & O. Vaselli (Eds.), Acta Vulcanol., 7, 1-13.

Csontos, L., Nagymarosy, A., Horváth, F. & Kovác, M. (1992): Tertiary evolution of the intra-Carpathian area: a model. Tectonophysics, 208, 221-241.

Downes, H., Seghedi, I., Szakács, A., Dobosi, G., Vaselli, O., James, D.E., Rigby, I.J., Thirlwall, M.F. Rex, D. & Pécskay, Z. (1995): Petrology and geochemistry of late Tertiary/ Quaternary mafic alkaline volcanism in Romania. Lithos, 35, 65-81.

Johnson, M.C., & Rutherford, M.J. (1989): Experimental

calibration of the aluminium-in-hornblende geobarometer with application to Long Valley Caldera (California) volcanic rocks. Geology, 17, 837-841.

Lindsley, D.H. (1983): Pyroxene Thermometry. Am. Mineral., 68, 477-493.

Mason, P.R.D. (1995): Petrogenesis of subduction-related magmatic rocks from the East Carpathians, Romania. Unpubl. PhD Thesis, University of London, 264pp.

Mason, P.R.D., Downes, H., Thirlwall, M., Seghedi, I., Szakcs, A., Lowry, D. & Mattey, D. (In Press): Crustal assimilation as a major petrogenetic process in East Carpathian Neogene to Quaternary continental margin arc magmas. J. Petrol.

Matthews, S.J., Jones, A.P. & Gardeweg, M.C. (1994): Lascar Volcano, Northern Chile; Evidence for steady-state disequilibrium. J. Petrol., 35, 401-432.

Pécskay, Z., Edelstein, O., Seghedi, I., Szakács, A., Kovacs, M., Crihan, M. & Bernád, A. (1995): Recent K-Ar Dating of Neogene-Quaternary calc-alkaline rocks in Romania. In: «Neogene and related magmatism in the Carpatho-Pannonian Region», H. Downes & O. Vaselli (Eds.), Acta Vulcanol., 7, 53-61.

Peltz, S., Vâjdea, E., Balogh, K. & Pécskay, Z. (1985): Contributions to the chronological study of the volcanic processes in the Călimani and Harghita Mountains (East Carpathians, Romania). D. S. Inst. Geol. Geofiz., 72, 323.

Rădulescu, D. & Săndulescu, M. (1973): The plate-tectonics concept and the geological structure of the Carpathians. Tectonophysics, 16, 155-161.

Roure, F., Roca, E. & Sassi, W. (1993): The Neogene evolution of the outer Carpathian flysch units (Poland, Ukraine and Romania): Kinematics of a foreland / fold-and-thrust belt system. Sedim. Geol., 86, 177-201.

Seghedi, I. (1987): A petrological study of the Călimani caldera. Unpubl. PhD Thesis. University of Bucharest, 161 pp.

Seghedi, I., Grabari, G., Ianc, R., Tanasescu, A. & Vajdea, E. (1986): Rb, Sr, Zr, Th, U, K Distribution in the Neogene Volcanics of the South Harghita Mountains. D.S. Inst. Geol. Geofiz, 70-71/1, 453-473.

Seghedi, I., Szakács, A., Udrescu, C., Stoian, M. & Grabari, G. (1987): Trace Elements Geochemistry of the Southern Harghita Volcanics (East Carpathians): Calc-Alkaline and Shoshonitic Associations. D.S. Inst. Geol. Geofiz, 72-73/1, 381-397.

Socolescu, M., Popovici D., Visarion M. & Rosca, V. (1964): Structure of the earth's crust in Romania as based on the gravimetric data. Rev. Roum. Géol. Géophys. Géogr. of (Sér. Géophys.), 8, 3.

Stănică, D., Stănică, M. & Pinna, E. (1990): Magnetotelluric soundings in the East Carpathians-Harghita area. Rev. Roum. Geophys., 30, 25-35.

Szabó, Cs., Harangi, Sz. & Csontos, L. (1992): Review of Neogene and Quaternary volcanism of the Carpathian-Pannonian region. Tectonophysics, 208, 243-256.

Szakács, A. & Seghedi, I. (1995): The Călimani-Gurghiu-Hargita volcanic chain, East Carpathians: Volcanological features. In: «Neogene and related magmatism in the Carpatho-Pannonian Region», H. Downes & O. Vaselli (Eds.), Acta Vulcanol., 7, 145-153.

Szakács, A., Seghedi, I. & Pécskay, Z. (1993a): Peculiarities of South Harghita Mts. as the terminal segment of the Carpathian Neogene to Quaternary volcanic chain. Rev. Roum. Geol., 37, 21-36.

Szakács, A., Seghedi, I., Pécskay, Z. & Karátson, D. (1993b): Time-space evolution pattern of the Neogene/Quaternary volcanism in the Harghita Mts., East Carpathians. Terra Abstracts, Supplement no. 1 to Terra Nova, 5, 567.

Wells, P.R.A. (1977): Pyroxene thermometry in simple and complex systems. Contrib. Mineral. Petrol., 62, 129-139.

Wood, B.J. & Banno, S. (1973): Garnet-orthopyroxene and orthopyroxene-clinopyroxene relationships in simple and complex systems. Contrib. Mineral. Petrol., 42, 109-124.

Wright, T.L. & Doherty, P.C. (1970): A linear programming and least squares computer method for solving petrological mixing problems. Geol. Soc. Am. Bull., 81, 1995-2008.